Journal of Electroceramics 6:1, 7–12, 2001

Pressure-Induced Pyrochlore-Perovskite Phase Transformation in PLZST Ceramics

JOON-HYUNG LEE

Department of Inorganic Materials Engineering, Kyungpook National University, Taegu 702-701, Korea Fax: 82-53-955-8179
E-mail: jhlee@icm.re.kr

YET-MING CHIANG

Department of Materials Science and Engineering, Massachusetts Institute of Technology, Cambridge, MA02139, U.S.A.
Fax: 1-617-253-6201 E-mail: ychiang@mit.edu

Submitted May 22, 2000; Revised September 18, 2000; Accepted September 22, 2000

Abstract. The influence of applied pressure on the pyrochlore-perovskite phase transformation in the PLZST system was studied. A stoichiometric and homogeneous ferroelectric PLZST pyrochlore powder was prepared by the coprecipitation and freeze-drying method. In the absence of applied pressure, the phase transformation from pyrochlore to perovskite occurred at temperatures above 550 °C, with 100% perovskite phase being obtained at 750 °C. Because the molar volume of the pyrochlore is larger than that of perovskite phase by 8.5%, applied pressure is expected to accelerate the pyrochlore-perovskite phase transformation. When the pyrochlore powder was uniaxially cold-pressed, the temperature for initiation of the phase transformation was lowered, and the rate of transformation was increased. This effect is interpreted as an increased nucleation frequency due to the defects created at particle contacts. For evaluation of pressure effects during annealing at elevated temperature, the powder was hot-pressed at various temperatures and pressures in air. Hot-pressing was found to greatly enhance the phase transformation rate. This is attributed to the additional $P \cdot \Delta V_{\text{molar}}$ driving force for the phase transformation provided by applied pressure.

Keywords: perovskite, pyrochlore, phase transformation, driving force, pressure

1. Introduction

Recently, the development of metastable pyrochlore and oxygen-deficient pyrochlore phases of $A_2B_2O_7$ or $A_2B_2O_{7-\delta}$ in Pb-perovskite thin films made at lower processing temperatures by various methods has been reported [1–3]. The oxygen partial pressure dependence of the pyrochlore-perovskite phase formation has also been reported, and showed that an O_2 annealing ambient stabilizes the oxygen-rich pyrochlore phase relative to the ferroelectric perovskite phase, while annealing in N_2 results in higher perovskite formation rates at lower temperature than O_2 annealing [4–6].

Despite having typically a higher oxygen concentration than the corresponding perovskite, the pyrochlore structure has a lower ion packing density. Table 1 compares lattice parameters and cell volumes for pyrochlore and perovskite phases in several Pb-based systems. During this transformation, one pyrochlore unit cell composed of 8 $A_2B_2O_{7-\delta}$ units converts to 16 ABO_3 perovskite unit cells. In the case of $PbTiO_3$, $Pb(Mg_{1/3}Nb_{2/3})O_3$ and $Pb(Zn_{1/3}Nb_{2/3})O_3$ systems, 10.2, 10.5, and 9.9% volume shrinkage is expected respectively upon the pyrochlore-perovskite phase transformation. Based on this observation, we can consider pressure as a method to promote the pyrochlore-perovskite phase transformation.

The simple application of hydrostatic pressure at constant temperature will increase the enthalpy of the lower density phase by the amount $P \cdot \Delta V_{\text{molar}}$, increasing the driving force for the phase transformation compared to that which is present at atmospheric pres-

sure. Moreover, it is known that reactions in the solid state are often accelerated by cold-working the material [14]. Nucleation may be easier in plastically deformed regions of the crystal lattice due to increased effective driving force or lowered activation energy for atomic diffusion [15]. External pressure applied to a pyrochlore powder is therefore expected to stimulate the phase transformation to perovskite.

In this work, the effect of cold-compaction and hot-pressing on the phase transformation from pyrochlore to perovskite was studied in PLZST, a family of perovskites of interest for actuation based on the electric field-forced phase transformation from the antiferroelectric tetragonal (A_T) to ferroelectric rhombohedral (F_R) phase [16]. The selected composition $Pb_{0.97}La_{0.02}(Zr_{0.64}Sn_{0.25}Ti_{0.11})O_3$ lies on the phase boundary between A_T and F_R phases. The effect of applied pressure on the pyrochlore-perovskite phase transformation was analyzed by using X-ray diffraction, SEM, and HRTEM.

2. Experimental

Homogeneous ultrafine powder of $Pb_{0.97}La_{0.02}(Zr_{0.64}Sn_{0.25}Ti_{0.11})O_3$ composition was synthesized by a coprecipitation method. $Pb(NO_3)_2$ (99.9%), $La(NO_3)_3{\cdot}6H_2O$ (99.99%), $ZrOCl_2{\cdot}8H_2O$ (99.9%), $SnCl_4$ (99.99%), and $TiCl_4$ (99.999%) were used as starting chemicals. For preparing the titanium and tin source solutions, $TiCl_4$ and $SnCl_4$ were dissolved in 30% aqueous H_2O_2 in a glove box to prevent the hydrolytic precipitation of each hydroxide, and the solutions were diluted to form a 0.1 mol dm^{-3} aqueous solution. $Pb(NO_3)_2$, $La(NO_3)_3{\cdot}6H_2O$, $ZrOC1_2{\cdot}8H_2O$ were dissolved in distilled water individually and diluted to a concentration of 0.1 mol dm^{-3}. The mixed solution corresponding to the composition of $Pb_{0.97}La_{0.02}(Zr_{0.64}Sn_{025}Ti_{0.11})O_3$ was kept below pH = 1 to avoid precipitation. The PLZST solution was added dropwise to a continuously stirred bath of NH_4OH solution whose pH was adjusted to 9, which was predicted by the solubility diagram as the optimum pH for the formation of a pure PLZST hydroxide precursor [13]. During the coprecipitation, the pH of the bath was maintained at 9 by adding NH_4OH solution as necessary, and the bath temperature was maintained at 60 °C in order to dissolve any lead and tin chlorides formed during the mixing process. After the precipitation, the bath was cooled to room temperature and held for 1 hour for equilibration. Then the precipitate was separated by decantation of the supernatant liquid, and washed several times with a distilled water—NH_4OH solution adjusted to pH 9—to remove residual $C1^-$ and NO_3^- ions. The precipitate was sprayed into liquid nitrogen and freeze dried in order to maintain chemical homogeneity and prevent powder agglomeration. The precipitate was then calcined. When the precipitate was calcined at 550 °C, ultra fine (diameter = 5 ∼ 8 nm) pyrochlore phase powder was formed, for which the phase transformation kinetics in the absence of applied pressure are known [13]. This pyrochlore phase powder was used as the starting material in this experiment. For the evaluation of cold-pressing effect on the pyrochlore-perovskite phase transformation, the pyrochlore powder was uniaxially cold-pressed into a disk under pressure of 310 MPa for 1 minute and annealed at 550 °C for various times. For evaluation of pressure effects during the transformation, the powder was hot-pressed at various temperatures (550 ∼ 750 °C) and 1 GPa pressure in air. Powder X-ray diffraction with nickel-filtered Cu-Kα radiation (Rigaku RTP 500 RC) was used for monitoring of phase development and identification. The volume fraction of pyrochlore and perovskite phases was determined by measuring the integrated intensity of (222) and (110) peaks for the two respective phases. SEM and HRTEM were also used for characterization of microstructure.

3. Results and Discussion

3.1. Effect of Cold-compaction on Phase Transformation

The starting pyrochlore phase powder is shown in Fig. 1. Ultrafine particles with 5 ∼ 8 nm diameter are observed in a well dispersed state. Lattice fringe are clearly seen in the HRTEM image, showing that the powders are well crystallized. X-ray diffraction (Fig. 2) shows broadened pyrochlore peaks attributed to the fine particle size.

Fig. 2 also shows X-ray diffraction patterns of the pyrochlore phase powder after annealing at 550 °C in the absence of applied pressure. Not until a calcining time of 8 h is reached does the perovskite peak near $2\theta \approx 31°$ become evident. Fig. 3 shows a series of X-ray diffraction patterns of the pyrochlore powder annealed at increasing temperatures for a fixed time of 1 h. With

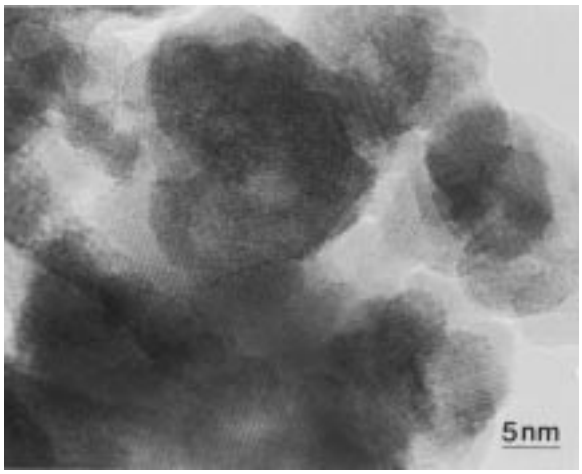

Fig. 1. HRTEM image of the starting pyrochlore powder.

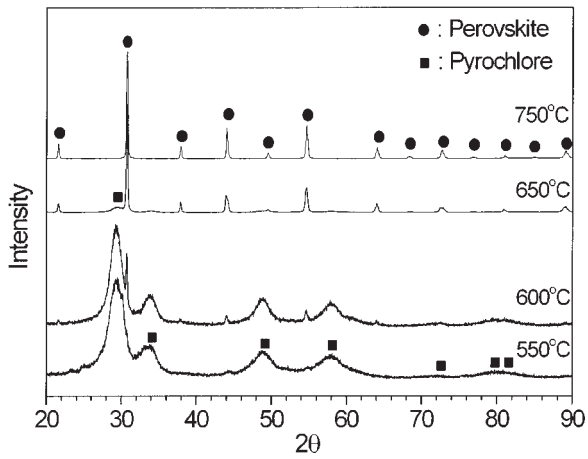

Fig. 3. X-ray diffraction patterns of the pyrochlore powder after calcining 1 h at increasing temperatures.

increasing annealing temperature, the perovskite PLZST phase begins to appear, and a single phase perovskite was obtained after firing at 750 °C for 1 h. At intermediate temperatures between 550 ~ 750 °C, pyrochlore and perovskite phases coexist. The kinetics of this transformation indicate a diffusion-limited process [13], for which Johnson-Mehl-Avrami analysis [17,18] gives an activation energy of 53.9 kcal/mol.

The starting pyrochlore powder was uniaxially cold pressed into a disk at room temperature with a pressure of 310 MPa for 1 minute and then annealed at 550 °C for various times. X-ray diffraction results in Fig. 4 show a large increase in the rate of phase transformation from pyrochlore to perovskite compared with those in Fig. 2. Note the sharpness of the perovskite peak, indicating a particle size ≥50 nm. We interpret the lowered phase transformation temperature and the increased phase transformation rate in the cold-pressed samples as being due to an increased nucleation frequency. Since particle contacts are regions of stress concentration where the local stress can be many times higher than the applied pressure [19], these are the likely nucleation sites.

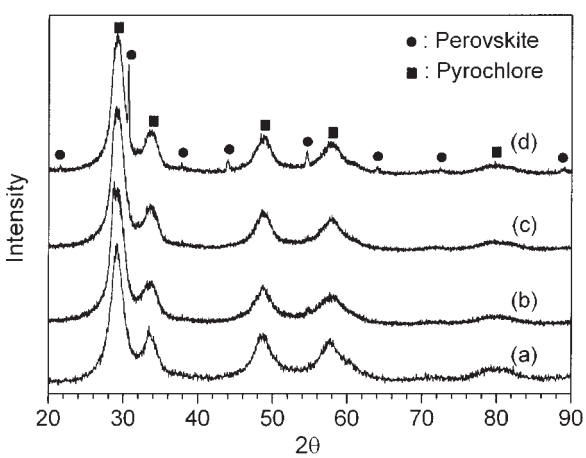

Fig. 2. X-ray diffraction patterns of pyrochlore powder as a function of annealing at 550 °C for (a) 1h, (b) 2h, (c) 4h, and (d) 8h.

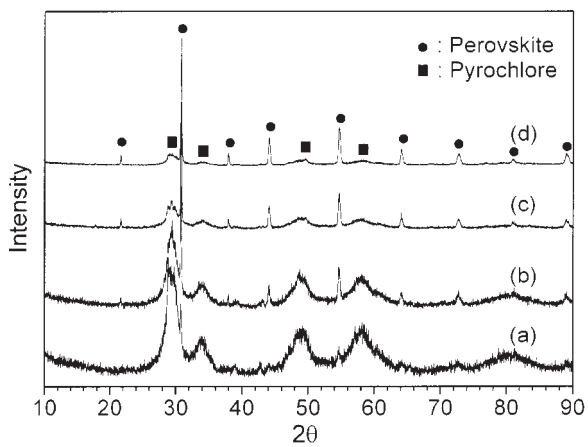

Fig. 4. X-ray diffraction patterns of cold-compacted pyrochlore powder as a function of annealing at 550 °C for (a) 1h, (b) 2h, (c) 4h, and (d) 8h.

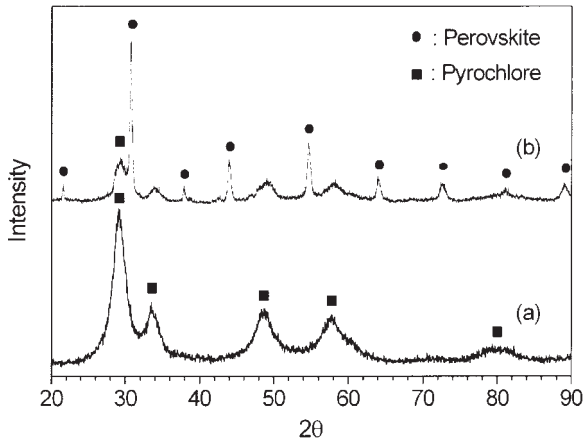

Fig. 5. X-ray diffraction patterns of pyrochlore powder, (a) loose powder annealed at 550 °C for 1 h, and (b) hot pressed at 550 °C for 1h under 1 GPa pressure.

3.2. Effect of Applied Pressure During Phase Transformation at Elevated Temperature

Hot-pressing further accelerated the pyrochlore to perovskite transformation. Fig. 5 compares X-ray diffraction patterns for the pyrochlore powder after a) annealing at 550 °C for 1h and b) hot-pressed at 1 GPa, 550 °C for 1h. Comparing with Fig. 4, it is obvious that the phase transformation has been further enhanced.

The volume fraction of perovskite phase as a function of temperature for loose and hot-pressed samples is shown in Fig. 6. These results were determined using the integrated intensity of pyrochlore (222) and perovskite (110) peaks, respectively. It is seen that the effect of hot-pressing is greatest at lower temperatures where essentially no transformation occurs in loose powders.

Fig. 7 shows the fracture surfaces of samples hot pressed at (a) 700 °C with a pressure of 500 MPa for 1h and (b) at 650 °C with a pressure of 1 GPa for 1h. In the sample hot pressed at the lower pressure of 500MPa, both fine pyrochlore phase powders (diameter ≈ 6∼8 nm) and perovskite grains (diameter ≈ 0.1 ∼0.3 μm) can be seen. At the higher pressure of 1 GPa, even though the temperature is 50°C lower, only

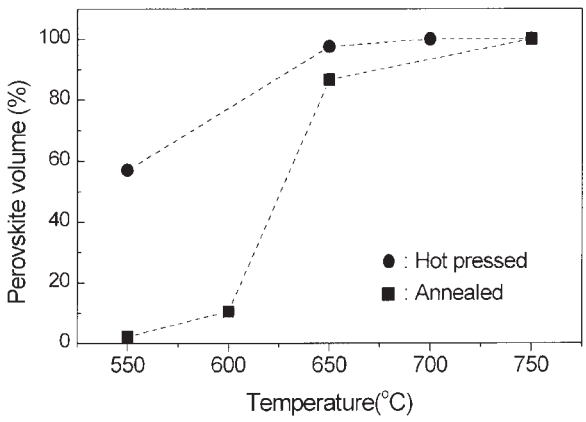

Fig. 6. Volume percent perovskite in loose and hot-pressed pyrochlore powder as a function of temperature for a fixed annealing time of 1 h.

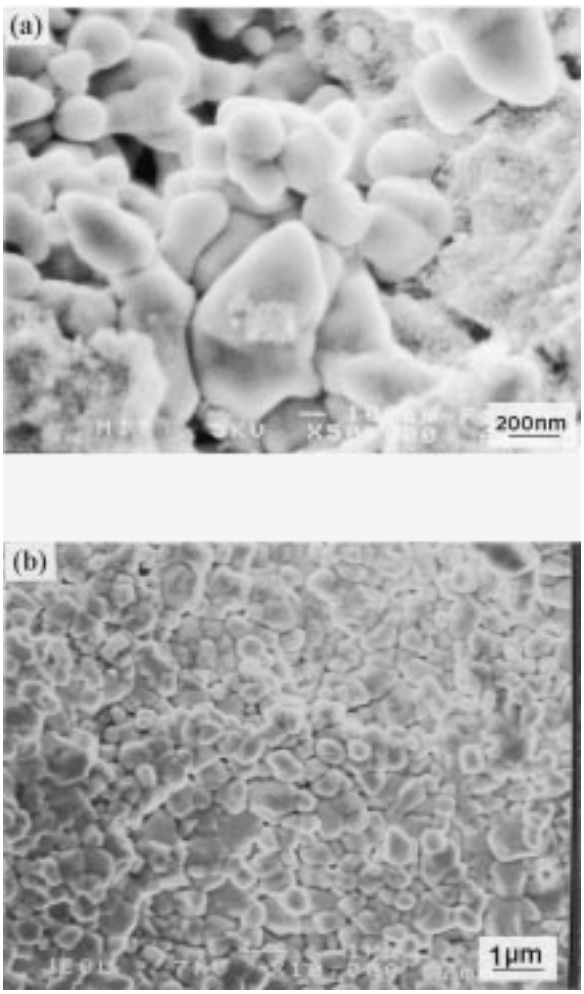

Fig. 7. Fracture surface of samples hot pressed at (a) 700 °C at 500 MPa in air for 1h, (b) 650 °C at 1 GPa in air for 1h.

Table 1. Calculated volume shrinkage for the pyrochlore-perovskite phase transformation in several systems.

	$PbTiO_3$		$Pb(Mg,Nb)O_3$		$Pb(Zn,Nb)O_3$		$(Pb,La)(Zr,Sn,Ti)O_3$ (This study)	
	Pyro[7]	Perov[8]	Pyro[9]	Perov[10]	Pyro[11]	Perov[12]	Pyro[13]	Perov[13]
Lattice parameters (Å)	a=10.40	a=3.899 c=4.153	a=10.59	a=4.049	a=10.60	a=4.062	a=10.67	a=4.112 α=89.84°
Molar volume (10^{-4} m^3/mol)	6.77	6.08	7.15	6.40	7.17	6.46	7.32	6.70
Volume shrinkage (%)	10.2		10.5		9.90		8.5	

perovskite grains (diameter 0.1 ∼ 0.7 μm) are seen. In the $Pb_{0.97}La_{0.02}(Zr_{0.64}Sn_{0.25}Ti_{0.11})O_3$ composition, the phase transformation from pyrochlore to perovskite has 8.5% volume shrinkage. (Table 1). Assuming a uniformly applied pressure (i.e., a densified sample), the increase in driving force for the phase transformation is $P \cdot \Delta V_{molar} = 14.7$ kcal/mol. In the early stage of hot-pressing before densification is complete, this increase is even greater at the particle contacts. In order to show that the $P \cdot \Delta V_{molar}$ driving force is responsible for the increased transformation rate, we annealed a sample that had been hot-pressed at 550 °C, 1 GPa for 1 h, in ambient pressure for increasing times up to 8 h. The X-ray diffraction patterns are shown in Fig. 8. Notice that no substantial increase in perovskite fraction is observed. Fig. 9 compares the perovskite volume fraction of these samples with those for loose powder annealed under identical conditions. The rate of transformation in the absence of applied pressure is approximately the same in both cases, showing that the $P \cdot \Delta V_{molar}$ driving force is responsible for accelerated phase transformation.

4. Conclusions

The pyrochlore to perovskite phase transformation has been shown to be promoted by both cold-compaction prior to annealing and by hot-pressing. The former effect is attributed to an increase in nucleation frequency due to defects at particle contacts. Enhanced phase

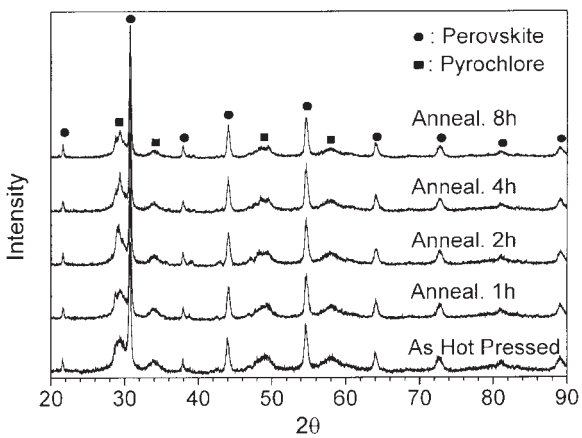

Fig. 8. X-ray diffraction patterns for samples first hot-pressed at 550 °C, 1 GPa for 1 h and then annealed at 550 °C for the times indicated.

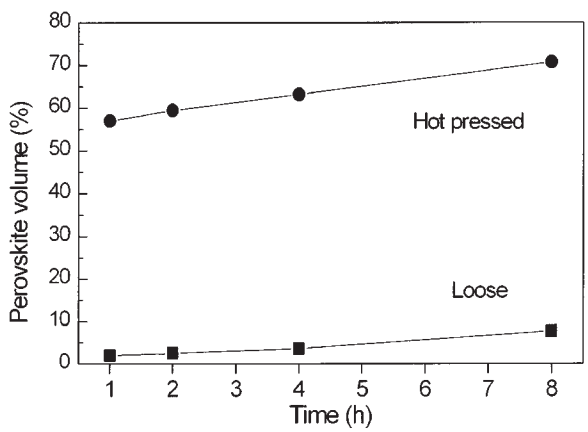

Fig. 9. Volume fraction perovskite in loose and hot-pressed samples as a function of annealing time at 550 °C.

transformation during hot-pressing is attributed to an increased $P \cdot \Delta V_{molar}$ driving force of approximately 14.7 kcal/mol. Both procedures represent simple but effective methods for increasing the transformation rate at reduced temperatures, such as is desired for producing fine-grained perovskite ceramics.

Acknowledgments

This work was supported by ARO-MURI Contact No. DAAH04-95-1-0104, and used instrumentation supported by the MRSEC Program of the National Science Foundation under award number DMR 98-08941. This work was also supported by post-doctoral fellowship from the Korea Science and Engineering Foundation (KOSEF).

References

1. S.A. Mansour, G.L. Liedl, and R.W. Vest, *J. Am. Ceram. Soc.*, **78,** 1617 (1995).
2. C.K. Kwok and S.B. Desu, in *Ceramic Transactions Vol. 25: Ferroelectric Films*, A.S. Bhalla and K.M. Nair, eds. (The American Ceramic Society, Westerville, OH, 1992), pp. 85.
3. C.H. Peng and S.B. Desu, *J. Am. Ceram. Soc.*, **77,** 1486 (1994).
4. L.A. Bursill and K.G. Brooks, *J. Appl. Phys.*, **75,** 4501 (1994).
5. G.R. Fox and S.B. Krupanidhi, *J. Mater. Res.*, **9,** 699 (1994).
6. K.G. Brooks, I.M. Reaney, R. Klissurska, Y. Huang, L. Bursill, and N. Setter, *J. Mater. Res.*, **9,** 2540 (1994).
7. JCPDS card #26-0142 for pyrochlore $Pb_2Ti_2O_6$.
8. JCPDS card #06-0452 for perovskite $PbTiO_3$.
9. JCPDS card #33-0769 and #37-0071 for pyrochlore $Pb_{1.83}Nb_{1.71}Mg_{0.29}O_{6.39}$.
10. JCPDS card #27-1199 for perovskite $Pb(Mg_{1/3}Nb_{2/3})O_3$.
11. JCPDS card #34-0374 for pyrochlore $Pb_{1.83}Nb_{1.71}Zn_{029}O_{6.39}$.
12. JCPDS card #22-0662 for perovskite $P(Zn_{1/3}Nb_{2/3})O_3$.
13. J.-H. Lee and Y.-M. Chiang, *J. Mat. Chem.*, *9*, 3107 (1999).
14. J.W. Christian, *The Theory of Transformations in Metals and Alloys*, 2nd ed. (Pergamon Press, Oxford, 1975), pp. 415, 459.
15. N.B. Hannay, *Treatise on Solid State Chemistry, Vol. 5 Changes of State* (Plenum Press, New York, 1982), pp. 81, 89.
16. D. Berlincourt, *IEEE Transactions on Sonics and Ultrasonics*, **13,** 116 (1966).
17. M. Avrami, *J. Chem. Phys.*, **7,** 1103 (1939).
18. M. Avrami, *J. Chem. Phys.*, **9,** 177 (1941).
19. R. L. Coble, *J. Appl. Phys.*, **41,** 4798 (1970).